



Sandia National Laboratories

Operated for the U.S. Department of Energy by

Sandia Corporation

Albuquerque, New Mexico 87123

Livermore, California 94551

date: July 1, 2013

to: Distribution

from: William Scherzinger, 1524, MS 0840

subject: Pressurization of a Ring in Plane Strain

A significant amount of attention has been placed on solving the problem of the failure of an internally pressurized cylinder subjected to heating. Ideally we would like to gain confidence in our ability to model problems of this type. This has been attempted by comparing complex boundary value problems to complex experiments. However, these types of comparisons should probably be done last. First our modeling capabilities for problems of this type should be better understood.

Along these lines this memo lays out a very specific boundary value problem and an approximate solution to that problem against which we can compare solutions from our solid mechanics codes. The problem chosen is the internal pressurization of a ring subjected to plane strain.

Problem

The internal pressurization of a ring in plane strain is representative of the larger problem we are trying to model. A schematic of the plane strain problem is shown in Figure 1. The ring is internally pressurized which causes the ring to expand. As the ring expands the thickness decreases. The circumferential stress in the ring balances the pressure. The internal pressure can be written as a function of the current radius of the ring, or alternatively the radial displacement of the ring. The hardening behavior and decreasing thickness will cause the pressure, as a function of the radial displacement, to reach a maximum and then decrease.

This behavior is modeled analytically and solved using a semi-analytic technique. The problem is first simplified by assuming that the ratio of the thickness to the radius is small. This allows us to assume plane stress in the radial direction along with plane strain in the

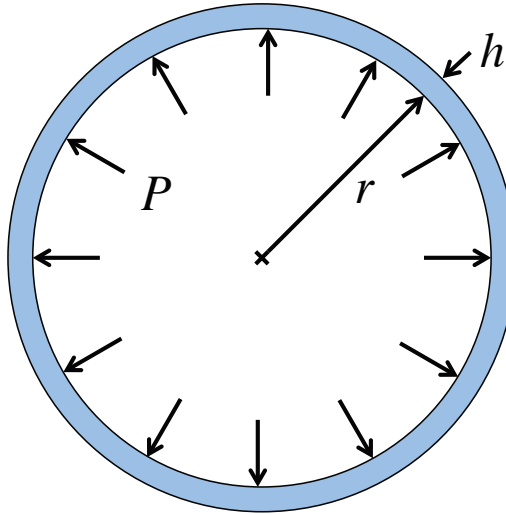


Figure 1. A schematic of a ring in plane-strain subjected to internal pressurization.

axial direction. Note that in this problem the assumption of plane stress is an approximation while the assumption of plane strain is exact.

For a semi-analytical solution to the problem we control the radial displacement. By controlling the radial displacement of the ring in the semi-analytical solution, we can calculate the entire pressure vs. radial displacement curve.

In the finite element model we can control the internal pressure. Given the nature of the maximum load we will arrive at a point where further solution is no longer possible. We can also control the radial displacement in the finite element model and back out the pressure from the circumferential stresses and the current thickness of the ring - just like we do with the semi-analytical solution. This allows us to find the solution past maximum load in the finite element problem.

Semi-Analytical Solution

We start by formulating the problem in cylindrical coordinates, (r, θ, z) , with the z -axis aligned with the axis of the ring. Since the problem only involves principal stresses and strains, we can write the Cauchy stress and logarithmic strains and strain rates as

$$\begin{aligned}
 \boldsymbol{\sigma} &= \sigma_r \mathbf{e}_r \mathbf{e}_r + \sigma_\theta \mathbf{e}_\theta \mathbf{e}_\theta + \sigma_z \mathbf{e}_z \mathbf{e}_z \\
 \boldsymbol{\varepsilon} &= \varepsilon_r \mathbf{e}_r \mathbf{e}_r + \varepsilon_\theta \mathbf{e}_\theta \mathbf{e}_\theta + \varepsilon_z \mathbf{e}_z \mathbf{e}_z \\
 \dot{\boldsymbol{\varepsilon}} &= \dot{\varepsilon}_r \mathbf{e}_r \mathbf{e}_r + \dot{\varepsilon}_\theta \mathbf{e}_\theta \mathbf{e}_\theta + \dot{\varepsilon}_z \mathbf{e}_z \mathbf{e}_z
 \end{aligned} \tag{1}$$

Assuming plane strain we have $\varepsilon_z = 0$ and $\dot{\varepsilon}_z = 0$. Making the plane stress assumption in the radial direction we have $\sigma_r = 0$.

For an initial radius, r_0 , and a current radius, r , the circumferential strain is

$$\varepsilon_\theta = \ln(r/r_0) = \ln(1 + u_r/r_0) \quad (2)$$

The current thickness of the ring, $h(r)$, is only a function of the current radius, r . The radial strain is

$$\varepsilon_r = \ln[h(r)/h_0] \quad (3)$$

where h_0 is the initial thickness.

The solution of the problem requires finding the circumferential and axial stress components, σ_θ and σ_z and the current thickness, h , as functions of the radial displacement. Once we solve for the circumferential stress and thickness, the pressure can be calculated as

$$P = \frac{h}{r} \sigma_\theta \quad (4)$$

The stress state has an elastic and an elastic-plastic solution. We start with the elastic solution.

For the elastic solution, Hooke's law in conjunction with $\varepsilon_z = 0$ can be used to show that the radial strain is related to the circumferential strain

$$\varepsilon_r = -\frac{\nu}{1-\nu} \varepsilon_\theta \quad (5)$$

where ν is the Poisson's ratio. Using (2) and (3) in (5) we get

$$h = h_0 \left(\frac{r}{r_0} \right)^{-\frac{\nu}{1+\nu}} \quad (6)$$

Using this in the linear elastic constitutive relation, with the Young's modulus E , we have

$$\sigma_\theta = \frac{E}{1-\nu^2} \varepsilon_\theta \quad ; \quad \sigma_z = \nu \sigma_\theta \quad (7)$$

The elastic solution is no longer applicable when the von Mises stress, $\bar{\sigma}$, is greater than the yield stress, σ_y . The von Mises stress for the elastic solution is given by

$$\bar{\sigma} = \sqrt{1 - \nu + \nu^2} \sigma_\theta \quad (8)$$

Once plastic deformation starts we must solve the plasticity equations subjected to plane-stress and plane-strain.

The elastic-plastic solution is most easily found by starting with the continuum tangent for an isotropic elastic-plastic material. We can find the continuum tangent from the equation for the stress rate

$$\dot{\boldsymbol{\sigma}} = \mathbb{C} : (\dot{\boldsymbol{\varepsilon}} - \dot{\boldsymbol{\varepsilon}}^p) \quad (9)$$

where \mathbb{C} is the tensor of elastic moduli

$$\mathbb{C} = \lambda \mathbf{I} \otimes \mathbf{I} + 2\mu \mathbf{II} \quad (10)$$

where λ and μ are the Lamé constants, \mathbf{I} is the second order identity tensor, \mathbf{II} is the fourth order symmetric identity tensor.¹ In (9) we have assumed an additive decomposition of the strain rate into an elastic and a plastic part. The yield surface for the model is defined by

$$f(\boldsymbol{\sigma}, \gamma) = \phi(\boldsymbol{\sigma}) - H(\gamma) \quad (11)$$

where γ is the hardening parameter. For the case of an isotropic plasticity model γ is equal to the equivalent plastic strain. The consistency condition requires $f \leq 0$. For plastic loading we require $\dot{f} = 0$

$$\frac{\partial \phi}{\partial \boldsymbol{\sigma}} : \dot{\boldsymbol{\sigma}} - H' \dot{\gamma} = 0 \quad (12)$$

The equivalent plastic strain is assumed to be associative

$$\dot{\boldsymbol{\varepsilon}}^p = \dot{\gamma} \frac{\partial \phi}{\partial \boldsymbol{\sigma}} \quad (13)$$

¹ $\mathbf{I} = \delta_{ij} \mathbf{e}_i \mathbf{e}_j$ and $\mathbf{II} = \frac{1}{2} (\delta_{ik} \delta_{jl} + \delta_{il} \delta_{jk}) \mathbf{e}_i \mathbf{e}_j \mathbf{e}_k \mathbf{e}_l$.

Substituting (9) and (13) into (12) we get

$$\frac{\partial\phi}{\partial\sigma} : \mathbb{C} : \dot{\epsilon} - \dot{\gamma} \frac{\partial\phi}{\partial\sigma} : \mathbb{C} : \frac{\partial\phi}{\partial\sigma} = H' \dot{\gamma} \quad (14)$$

Which can be solved for $\dot{\gamma}$

$$\dot{\gamma} = \frac{\frac{\partial\phi}{\partial\sigma} : \mathbb{C} : \dot{\epsilon}}{\frac{\partial\phi}{\partial\sigma} : \mathbb{C} : \frac{\partial\phi}{\partial\sigma} + H'} \quad (15)$$

Using (13) and (15) in (9) we get

$$\dot{\sigma} = \left[\mathbb{C} - \frac{\frac{\partial\phi}{\partial\sigma} : \mathbb{C} : \frac{\partial\phi}{\partial\sigma}}{\frac{\partial\phi}{\partial\sigma} : \mathbb{C} : \frac{\partial\phi}{\partial\sigma} + H'} \right] : \dot{\epsilon} \quad (16)$$

Specializing for the case of an isotropic plasticity model where

$$\phi(\sigma) = \sqrt{\frac{3}{2} \mathbf{s} : \mathbf{s}} \quad ; \quad \mathbf{s} = \sigma - \frac{1}{3} (\text{tr}\sigma) \mathbf{I} \quad (17)$$

we get

$$\dot{\sigma} = \left[\mathbb{C} - \frac{2\mu}{1 + H'/3\mu} \mathbf{N} \otimes \mathbf{N} \right] : \dot{\epsilon} \quad (18)$$

where H' is the slope of the hardening curve at a given plastic strain. The normal tensor, \mathbf{N} , is

$$\mathbf{N} = \frac{\mathbf{s}}{\|\mathbf{s}\|} \quad (19)$$

The relationship between the radial and circumferential strain rates are found by setting $\dot{\sigma}_r = 0$ in (18). We denote the principal components of the normal, \mathbf{N} , as N_r , N_θ , and $N_z = -N_r - N_\theta$, and define a parameter, B , as follows

$$B = \frac{N_r}{1 + H'/3\mu} \quad (20)$$

If we denote the bulk modulus by K we can calculate the relationship between the radial and circumferential strain rates during plastic deformation as

$$\dot{\varepsilon}_r = - \left[\frac{3K - 2\mu(1 + 3BN_\theta)}{3K + 2\mu(2 - 3BN_r)} \right] \dot{\varepsilon}_\theta \quad (21)$$

This is solved using a forward Euler algorithm incrementing the radial displacement with very small steps to reduce the error. Given that this is a specific problem we are trying to solve, efficiency was not of primary importance. Once the strain rates are found then the stresses are updated using (18).

For comparisons to a finite element model the following constitutive model and parameters are chosen along with the geometry of the ring. *The parameters that are used are not meant to be for any real system.*

For the constitutive model, we use an elastic-plastic power law hardening model. The Young's modulus and Poisson's ratio for the elastic response of the material are chosen to be $E = 10 \times 10^6$ psi and $\nu = 0.25$. For the plastic response the power law hardening rule is

$$\bar{\sigma} = \sigma_y + A\bar{\varepsilon}_p^n \quad (22)$$

The properties for this hardening model are $\sigma_y = 10^4$ psi, $A = 10^4$ psi and $n = 0.2$.

For the geometry of the ring, an outer radius of 10 in. is used. The inner radius is 9.99 in., giving a thickness of 0.01 in. and a thickness to radius ratio of 0.001. The pressure-displacement curve for the semi analytical solution for this geometry and material are shown in Figure 2

Finite Element Model

The semi-analytical solution is used to see if the finite element solutions of a similar problem finds the same maximum load. The finite element model problem is an internally pressurized axisymmetric thin-walled ring under load control or displacement control. For the load control problem the model should fail to converge at maximum load. For a displacement control problem we expect to be able to solve the problem past maximum load.

Geometry and Material Model

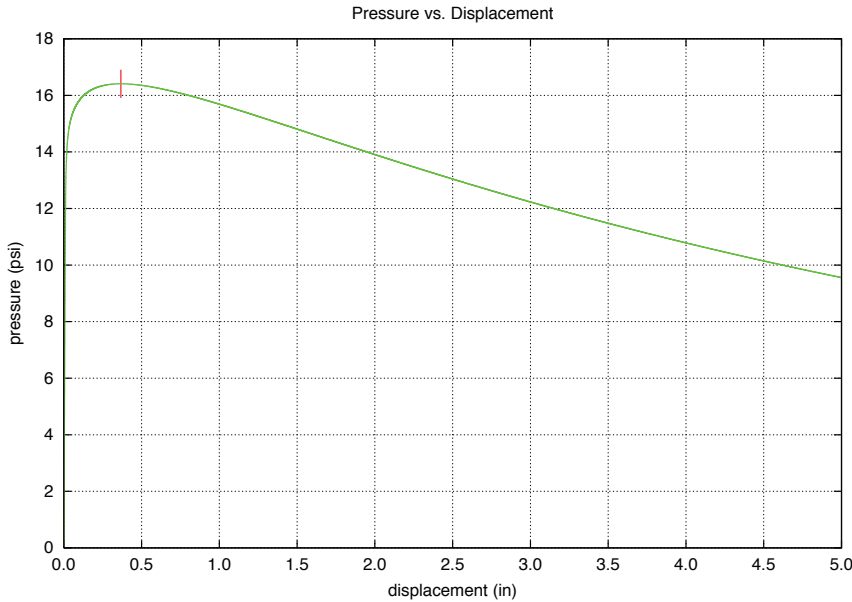


Figure 2. Pressure vs. radial displacement for a thin ring in plane strain. The red mark is the maximum load, which occurs at a pressure of 16.4 psi and a radial displacement of 0.367 in.

The geometry for the ring is the same as the geometry for the semi-analytical model. Since the model is a thin ring it should approximate the assumptions made in the semi-analytical solution, specifically the plane stress assumption.

The finite element model is a 30 degree wedge and has 5 elements through the thickness of the ring and one element in the axial direction - the direction where plane strain is enforced. Each element is approximately a cube 0.002 inches on each side. There are 13,085 elements and 31,416 nodes in the model.

The material model used for the finite element problem is the same as the model used for the semi-analytical model.

Load Control

For load control a surface is defined on the inner surface of the ring. This surface is used to apply a pressure boundary condition for the problem. The pressure is ramped with the function $p(t) = 20.0t$ psi, where t is the "time" in the analysis. The time scale for this problem does not matter since the model is rate independent and the solution is assumed to be quasi-static. Therefore the time in the solution is a non-dimensional loading function. If we were to look at any rate dependent constitutive model then the time scale would have to

be adjusted to be relevant to the time scales in the specific model.

Displacement Control

For displacement control a radial displacement is prescribed for the inside surface of the ring. The loading function is $d(t) = 5.0t$ inches. Once again the time scale in this boundary value problem can be considered a non-dimensional loading parameter.

Results

The results for the finite element model are shown in Figure 3. Here the results are plotted for load control and displacement control, and compared to the semi-analytical pressure vs. displacement curve and the maximum pressure from the semi-analytical solution.

For the load control case, an internal pressure is applied to the inside surface of the ring. This is increased until the model fails to converge. This occurs at maximum load. The finite element solution under load control is seen to agree with the semi-analytical solution up to the maximum load. Beyond the maximum pressure the finite element solution fails to

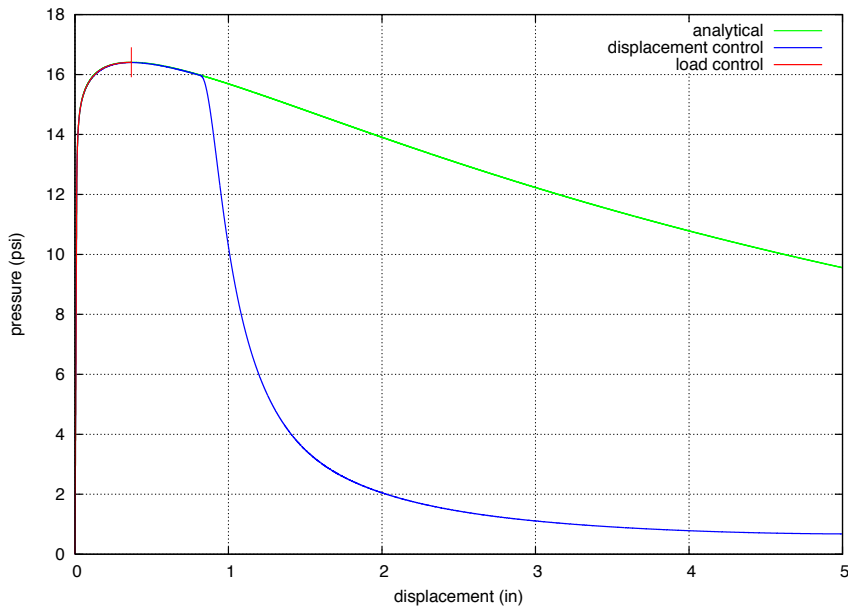


Figure 3. Finite element results showing pressure vs. radial displacement for a thin ring in plane strain. Two problems are run: load (pressure) control and displacement control. Load control can only be run up to maximum load (the red line) while displacement control can be run past maximum load. The onset of necking *appears* to be captured for this problem using displacement control.

converge. This is obvious since, if we are monotonically increasing the pressure, there is no solution for a pressure larger than the maximum load.

For the displacement control problem a radial displacement is prescribed for the inside surface of the ring. The pressure is calculated from the current circumferential stress, ring thickness and mean radius of the ring. For displacement control the problem converges nicely past maximum load until what might be the onset of necking. In some cases necking is captured by Adagio, and in some cases it fails to capture it. Modifying the problem slightly can cause the finite element model to simply fail to converge at some point past maximum load. Therefore we must be hesitant to ascribe the change in the behavior of the pressure-displacement curve to a physically meaningful necking instability without performing a proper stability analysis. ***No conclusions will be drawn in this memo about instabilities that may exist past maximum load.*** With the proper computational tools that would allow us to check for bifurcation and the post-bifurcation solution, then we could make a definite statement about necking and localization. Examining necking and localization in more detail could provide a very useful study for future work.

Conclusions

Our solid mechanics finite element code, Adagio, is capable of predicting the maximum pressure for the problem of an internally pressurized ring in plane strain. The problem can be modeled using load control or displacement control. If load control is used then the solution can not be continued past maximum load. Depending on the particular problem that one wishes to model, load or displacement control might be appropriate.

This problem gives us confidence that we can also model the behavior of an internally pressurized cylinder. The model problem can also be extended to look at the behavior of more complicated problems. Models that include temperature dependence, rate dependence or anisotropy are examples of models we would want to consider.

However, we will see behavior in an internally pressurized cylinder that is not seen here. That model will exhibit non-uniform radial displacements in the axial direction, along with the possibility of bulging. Furthermore, additional modes of instability are available to an internally pressurized cylinder when compared to a ring. Finally, controlling the problem in such a way as to capture the post maximum load behavior will require new solution strategies in Adagio. These solution strategies might include an arc length method or a way to do volume control on the volume inside the cylinder.

Internal Distribution:

MS0344	J. F. Dempsey	1526
MS0346	D. E. Peebles	1526
MS0380	J. Jung	1542
MS0380	K. H. Pierson	1542
MS0812	N. L. Breivik	1524
MS0812	E. Corona	1524
MS0812	K. W. Gwinn	1524
MS0812	V. R. Romero	1544
MS0825	M. Pilch	1514
MS0832	W. R. Witkowski	1544
MS0840	H. E. Fang	1524
MS0840	K. N. Long	1524
MS0840	B. Reedlun	1524
MS1398	M. K. Neilsen	1526
MS9042	B. R. Antoun	8256
MS9042	A. Brown	8259